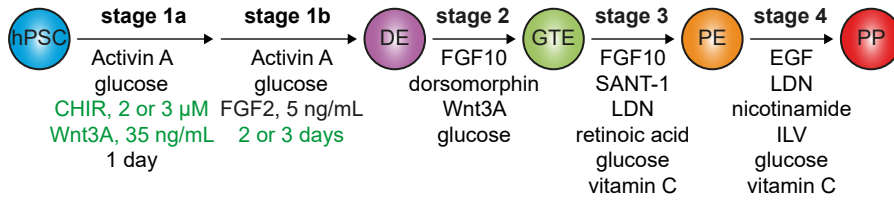


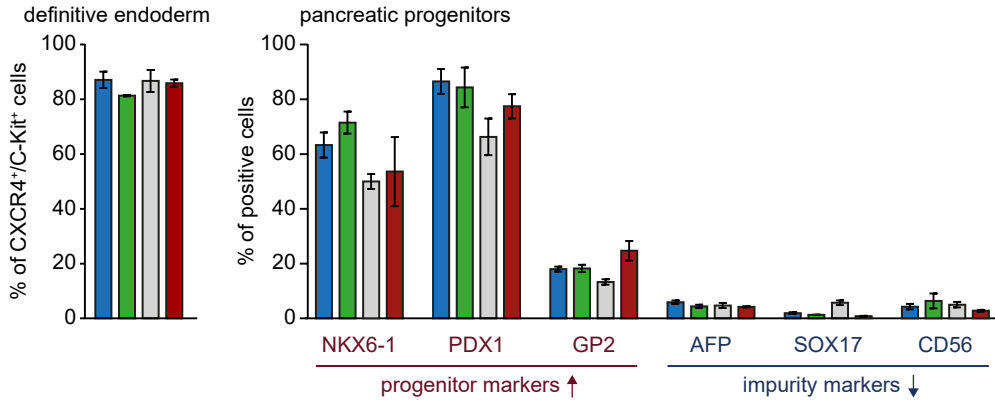
Figure S1. Overview of established protocols for the four-step PP generation with DE, GTE and PE as intermediate stages. Protocols from (A) Breunig et al. [1, 2], (B) Hohwieler et al. [3], (C) Hoglebe et al. [4], (D) Leite et al. [5] and (E) Mahaddalkar et al. [6] are depicted. (F) UMAPs showing the expression of *NKX6-1*, *PDX1*, *PTF1A*, and *SOX9* across the 5 clusters of a published single cell RNA sequencing data set (Hoglebe et al. [7]). CHIR: CHIR99021; DE: definitive endoderm; GTE: gut tube endoderm; ILV: Indolactam V; PE: pancreatic endoderm; PP: pancreatic progenitor

A

individual compound testing of stage 1



B



stage 1a

stage 1b

■	Activin A	glucose	CHIR	1 day	Activin A	glucose	FGF2	2 days
	100 ng/mL	4.4 mM	2 μM		100 ng/mL	4.4 mM	5 ng/mL	
■	Activin A	glucose	CHIR	1 day	Activin A	glucose	FGF2	2 days
	100 ng/mL	4.4 mM	3 μM		100 ng/mL	4.4 mM	5 ng/mL	
□	Activin A	glucose	Wnt3A	1 day	Activin A	glucose	FGF2	2 days
	100 ng/mL	4.4 mM	35 ng/mL		100 ng/mL	4.4 mM	5 ng/mL	
■	Activin A	glucose	CHIR	1 day	Activin A	glucose	FGF2	3 days
	100 ng/mL	4.4 mM	2 μM		100 ng/mL	4.4 mM	5 ng/mL	

Figure S2. Stage 1 compound testing reveals minor influence on PP generation. (A) Schematic overview of the individual compound testing for optimization of stage 1. The tested compounds are highlighted in red. (B) Flow cytometry results of CXCR4/C-KIT staining at definitive endoderm (DE) and of progenitors (NKX6-1, PDX1, GP2) and impurity markers (AFP, SOX17, CD56) at the pancreatic progenitor (PP) stage. The condition highlighted in red was used in the final protocol. Compounds that are written *in italics* were not varied. Mean, n=3. CHIR: CHIR99021; GP2: glycoprotein 2; GTE: gut tube endoderm; ILV: Indolactam V; LDN: LDN-193189; PE: pancreatic endoderm; VIM: vimentin

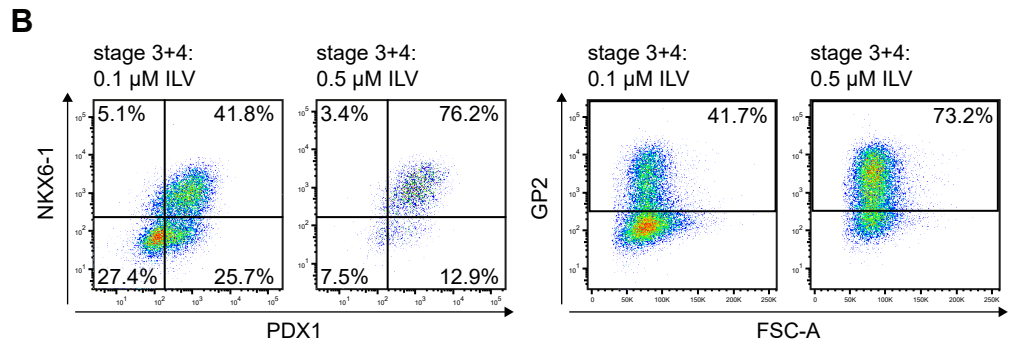
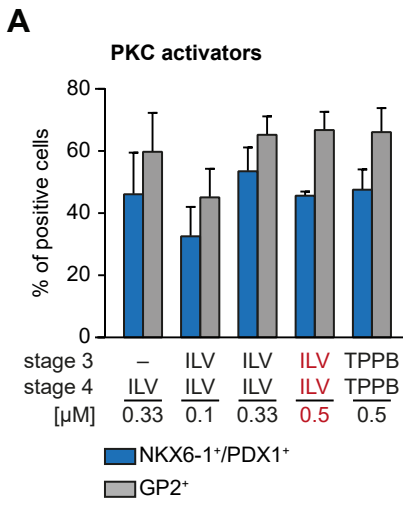
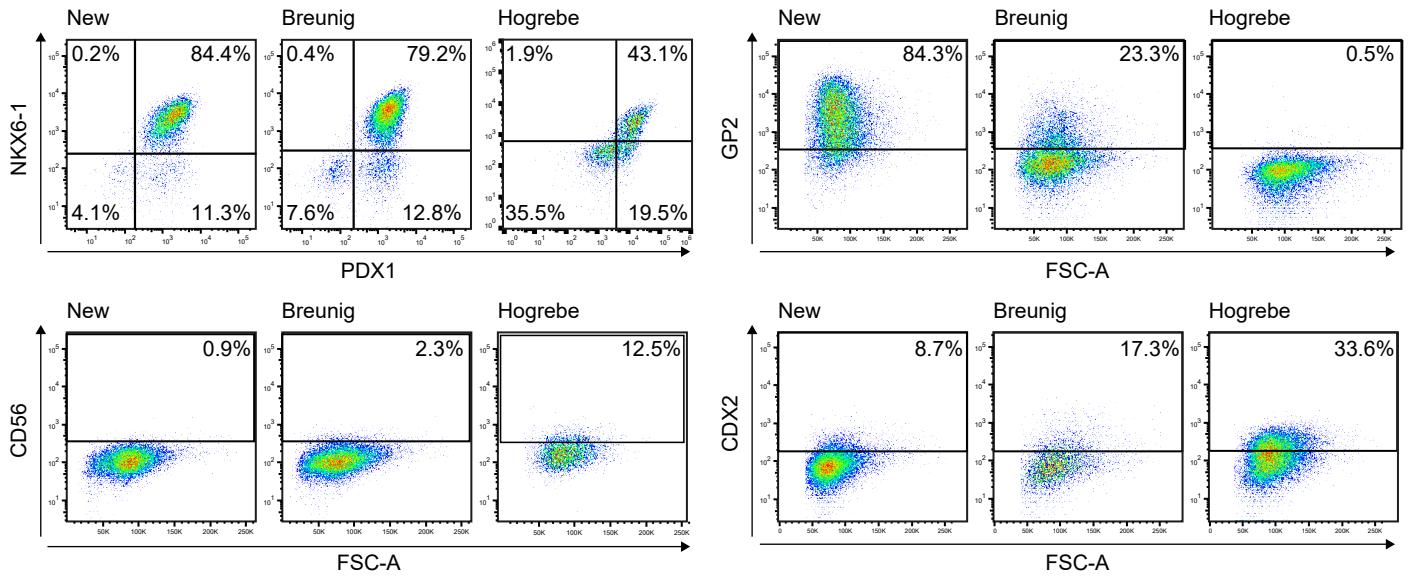


Figure S3. Influence of PKC activation on pancreatic progenitor generation. (A) Different concentrations and combinations of the PKC activators ILV (0.1 μ M, 0.33 μ M, 0.5 μ M) and TPPB (0.5 μ M) were analyzed in a separate experiment. Flow cytometry results of NKX6-1/PDX1 double positive population and GP2 positive cells are depicted. Mean \pm SEM, n=3. Significance was evaluated with two-way ANOVA, P < 0.05: *, p < 0.01: **, p < 0.001: ***. (B) Representative flow cytometry plots of NKX6-1/PDX1 and GP2 staining for various combinations and concentrations of PKC activators TPPB and ILV. GP2: glycoprotein 2; ILV: Indolactam V; PKC: protein kinase C

A



B

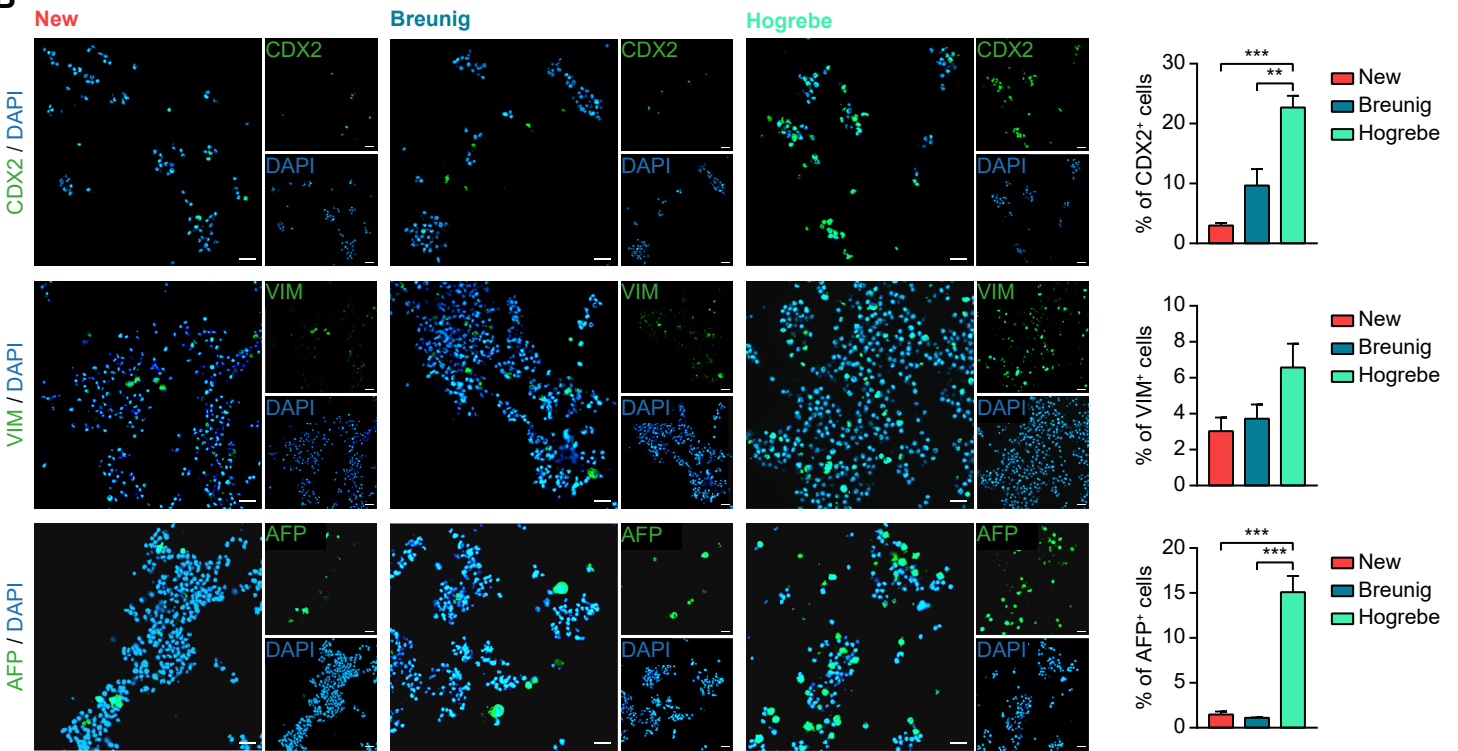
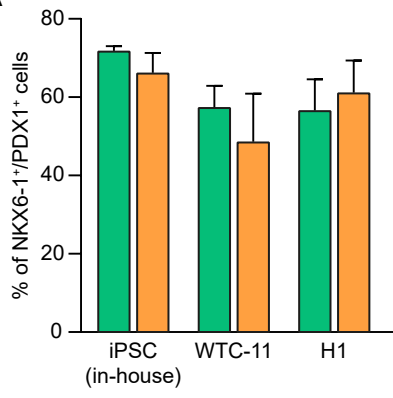
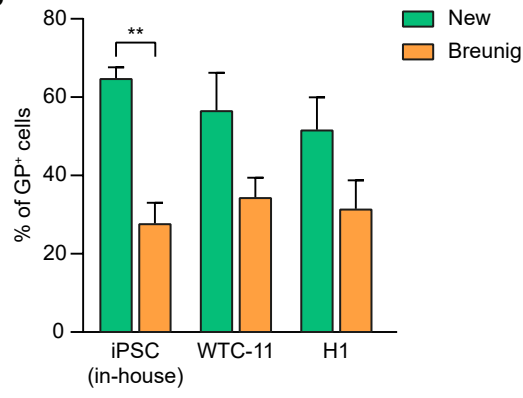


Figure S4. Characterization of pancreatic progenitors. (A) Representative flow cytometry plots of NKX6-1/PDX1, GP2, CD56 and CDX2 staining of PPs generated with the new, Breunig [1, 2] and Hoglebe [4] protocol. (B) Representative immunofluorescence stainings of the impurity markers CDX2 (green), VIM (green), and AFP (green) are shown along with their quantifications. CDX2 (n=4 fields of view), VIM (n=3 fields of view) and AFP (new n=3, Breunig n=3, Hoglebe n=4 fields of view) positive cells were normalized to DAPI. Scale bars represent 50 μ m. Significance was assessed with an ordinary one-way ANOVA, P < 0.05: *, p < 0.01: **, p < 0.001: ***. GP2: glycoprotein 2; PP: pancreatic progenitor; VIM: vimentin

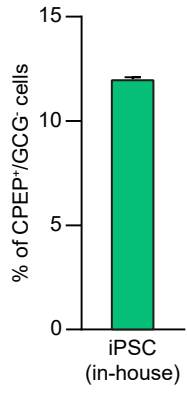
A



B



C



D

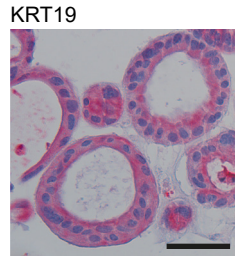
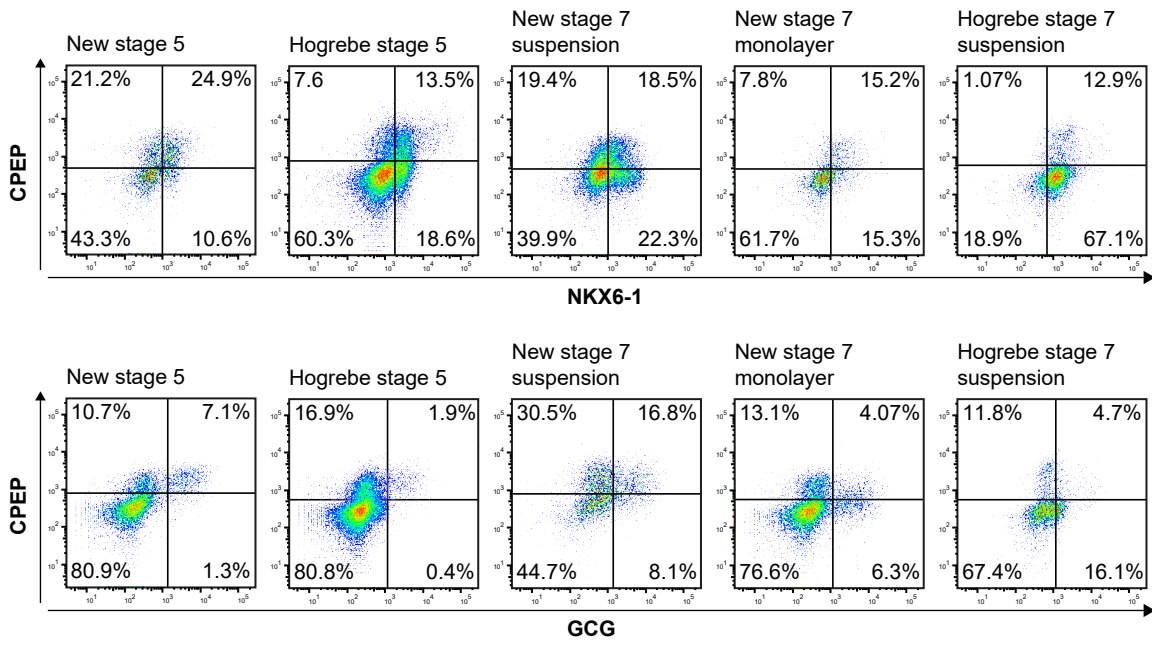


Figure S5. Elevated GP2 expression upon PP generation with the new protocol is reproducible across various cell lines. An in-house generated iPSC line, WTC iPSC line and H1 hESC line were differentiated to pancreatic progenitors using the new or Breunig protocol [1, 2]. **(A)** FC analysis results of NKX6-1 and PDX1 double positive population and **(B)** GP2 positive cells are shown. Bars represent mean \pm SEM, n=6 (in-house iPSC, H1) or n=4 (WTC). Significance was determined with two-tailed t-test, P < 0.05: *, p < 0.01: **, p < 0.001: ***. **(C)** Bar graph shows the CPEP⁺/GCG⁻ cells (flow cytometry) of endocrine progenitors generated by applying the new protocol to an in-house generated iPSC line in technical duplicates. **(D)** Ductal differentiation with the new protocol of an in-house generated iPSC line was shown with IHC staining of KRT19. Scale bars represent 50 μ m. GP2: glycoprotein 2; iPSC: induced pluripotent stem cell

A



B

endocrine progenitors (stage 5)

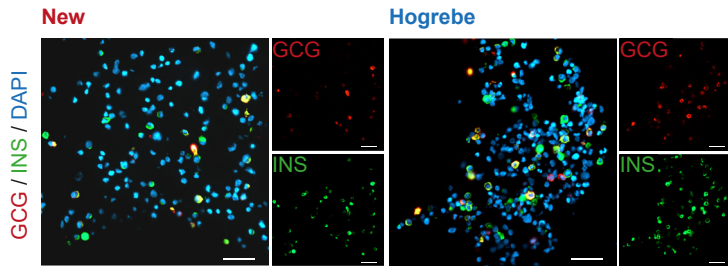


Figure S6. Characterization of stem-cell derived endocrine cells. (A) Representative FC plots (NKX6-1/CPEP, GCG/CPEP) at the endocrine stage 5 and stage 6 of cells generated with the new or Högberg [4] protocol are shown. (B) Immunofluorescence staining for GCG (red) and INS (green) of endocrine progenitors (stage 5). Counterstaining was performed with DAPI (blue). Scale bars represent 100 μm . CPEP: c-peptide; GCG: glucagon; INS: insulin

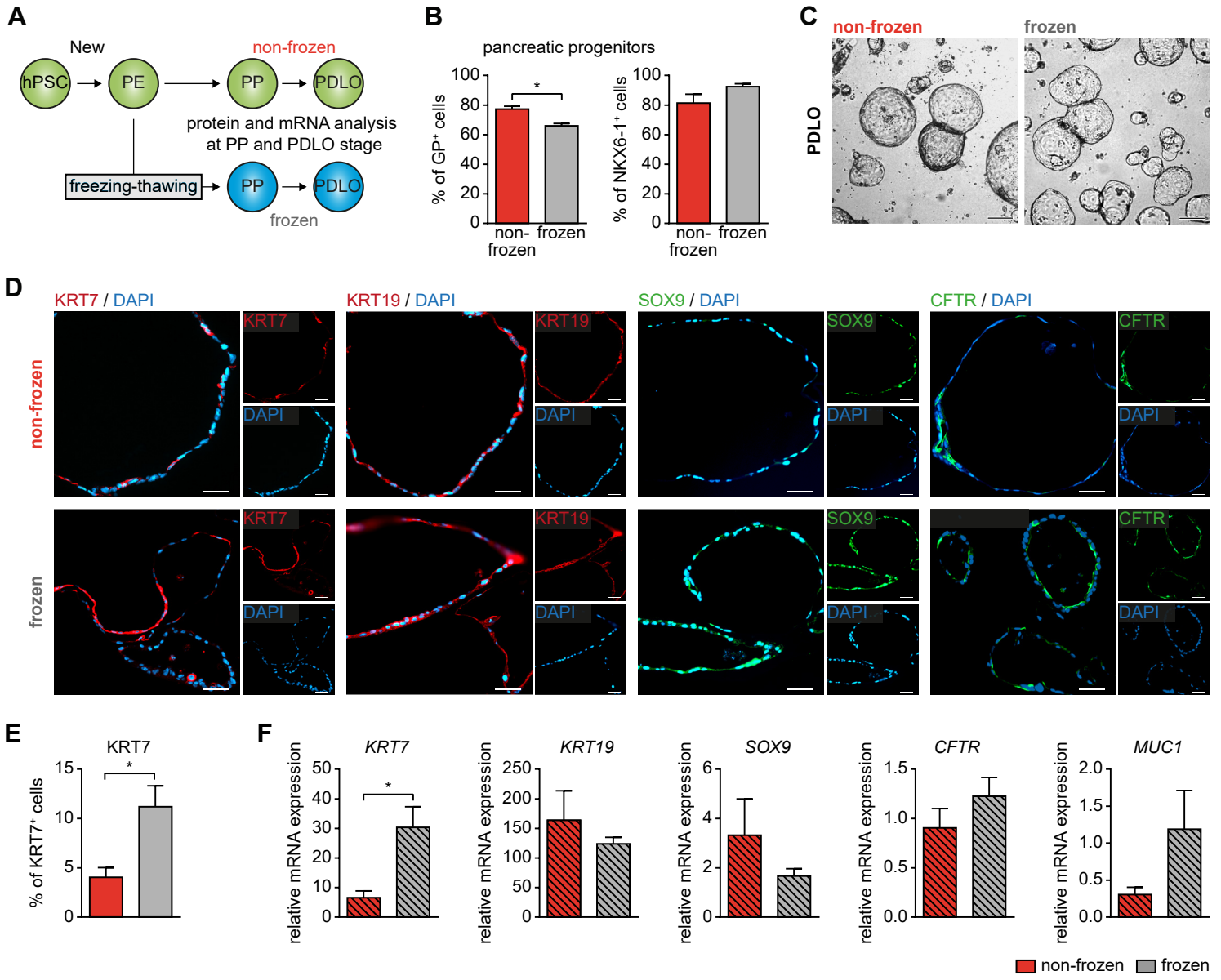


Figure S7. *In vitro* ductal differentiation of new pancreatic progenitors is improved through a freeze-thaw cycle at pancreatic endoderm stage. (A) Schematic illustration of PP differentiation according to the new protocol and further ductal commitment, with a freeze-thaw cycle at PE stage. (B) Evaluation of the progenitor markers GP2 and NKX6-1 at PP stage by flow cytometry. (C) Brightfield images of PDLOs derived from frozen and non-frozen PE cells. (D) Immunofluorescence staining of ductal organoids shows expression of the ductal markers KRT7 (red), KRT19 (red), SOX9 (green), and CFTR (green). Cells were counterstained with DAPI (blue). (E) Flow cytometry of KRT7 is shown. (F) mRNA levels of the ductal markers *KRT7*, *KRT19*, *SOX9*, *CFTR*, and *MUC1* were measured by qPCR. All gene expression data were normalized to the housekeeping gene *HMBS*. Bar graphs depict mean \pm SEM, n=3. Significance was evaluated with two-tailed t-test, P < 0.05: *, p < 0.01: **, p < 0.001: ***. Scale bars of brightfield and immunofluorescence images represent 200 μ m and 100 μ m, respectively. GP2: glycoprotein 2; hPSC: human pluripotent stem cell; KRT19: keratin 19; KRT7: keratin 7; PDLO: pancreatic duct-like organoid; PE: pancreatic endoderm; PP: pancreatic progenitor

Figure S8

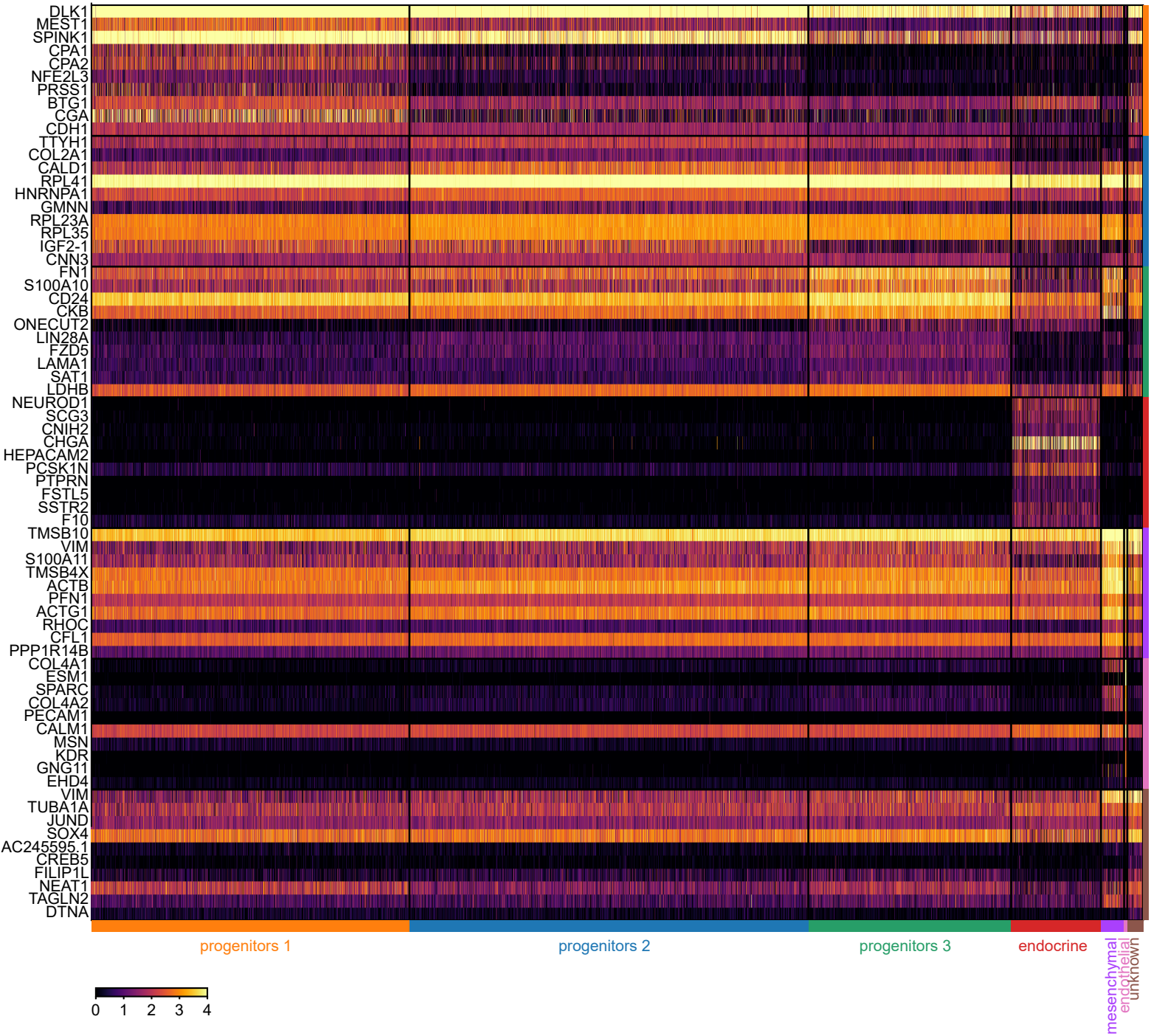


Figure S8. Top 10 cluster-defining differentially expressed genes. Heatmap showing the top 10 differentially expressed genes specifying each cell cluster of the single-cell transcriptome of new PPs. The respective gene expression for the individual cells is shown.

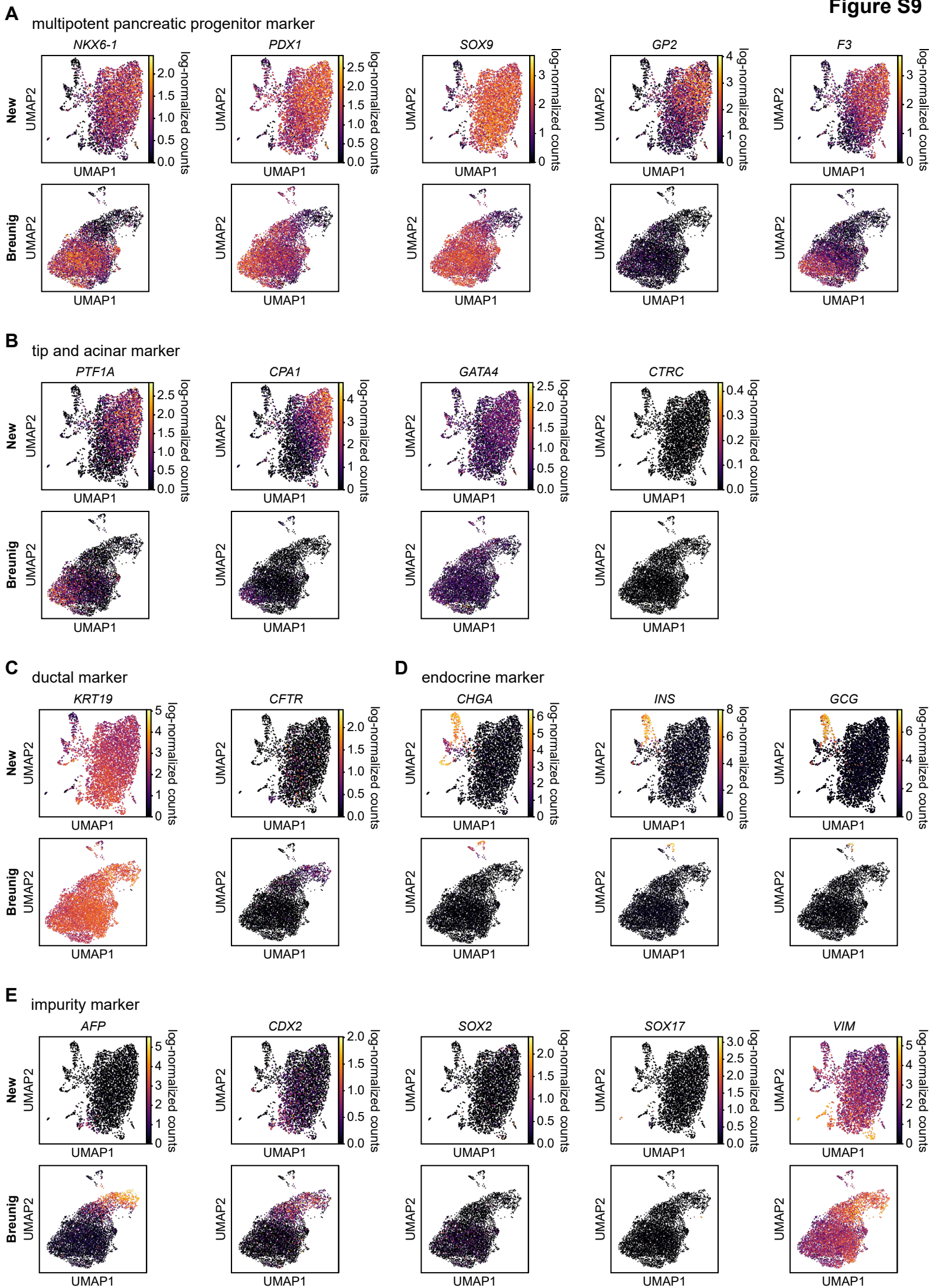


Figure S9. Marker distribution within single-cell datasets of pancreatic progenitors. UMAP plots of single-cell transcriptomes within pancreatic progenitors (new and Breunig) display the expression of (A) multipotent pancreatic progenitor markers (*NKX6-1*, *PDX1*, *GP2*, *SOX9*, *F3*), (B) tip and acinar markers (*PTF1A*, *CPA1*, *GATA4*, *CTRC*), (C) ductal markers (*KRT19*, *CFTR*), (D) endocrine markers (*CHGA*, *INS*, *GCG*), and (E) non-pancreatic impurity markers (*AFP*, *CDX2*, *SOX2*, *SOX17*, *VIM*). CHGA: chromogranin A; CPA1: carboxypeptidase 1; CTRC: chymotrypsin C; GCG: glucagon; GP2: glycoprotein 2; INS: insulin; KRT19: keratin 19; VIM: vimentin

Figure S10

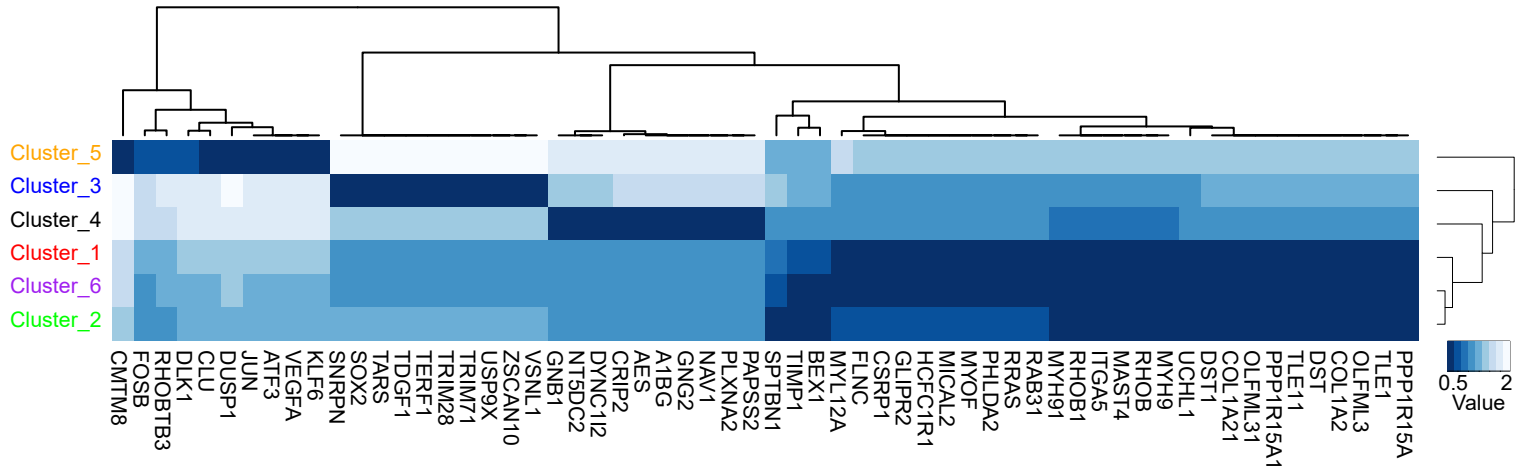
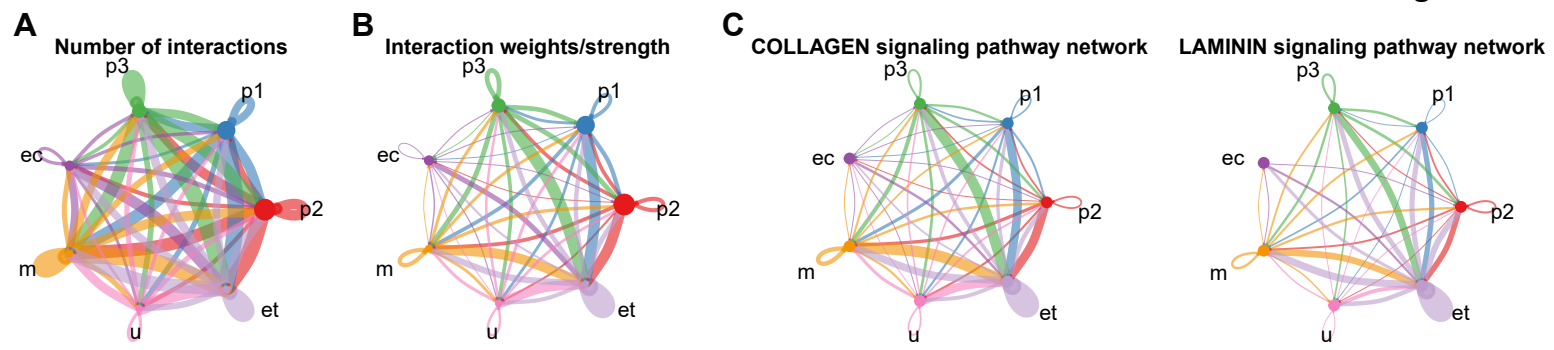


Figure S10. Comparison of a pancreatic progenitor dataset with a human fetal pancreas dataset leading to new cluster membership. Heatmap showing top 10 genes defining each cluster.



p1: progenitors 1; p2: progenitors 2; p3: progenitors 3; ec: endocrine; m: mesenchymal; u: unknown; et: endothelial

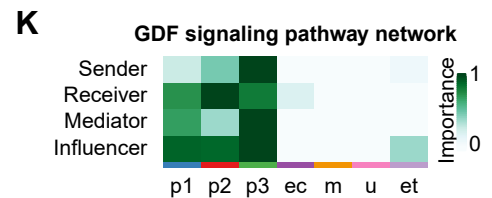
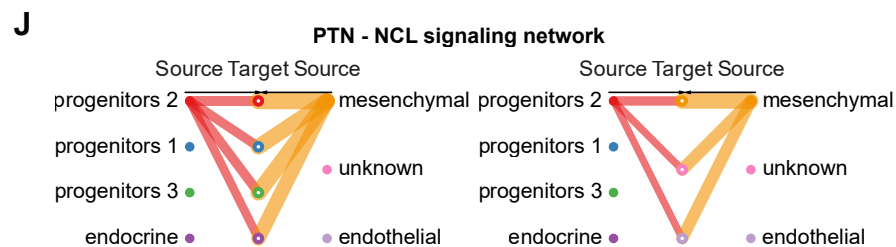
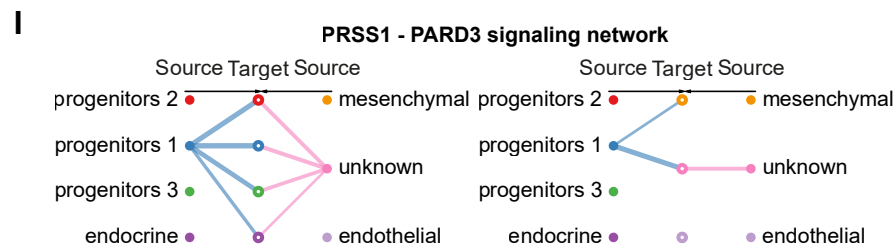
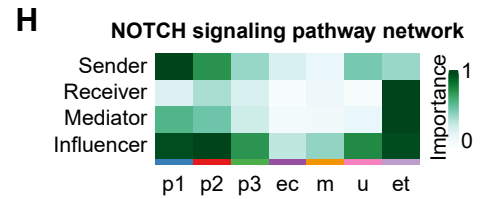
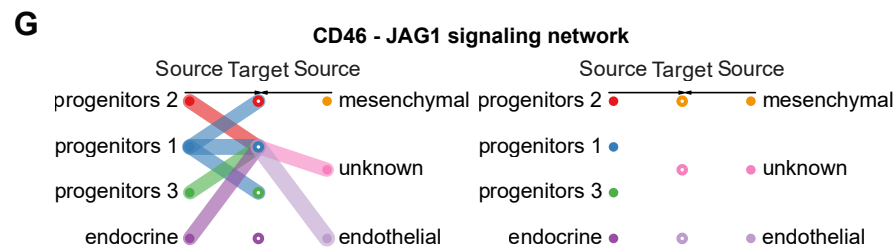
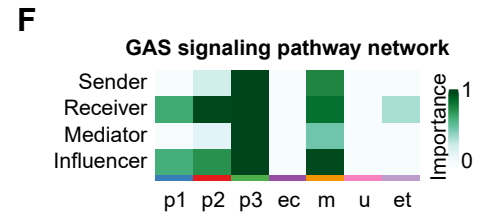
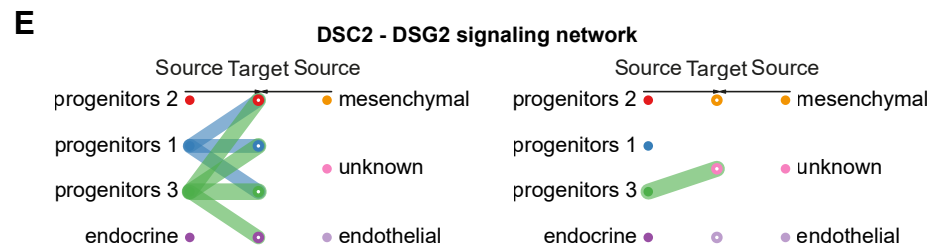
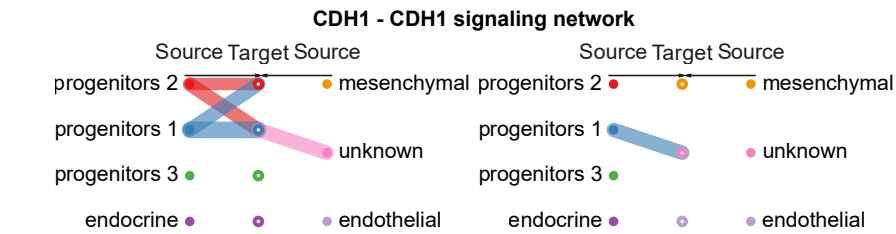
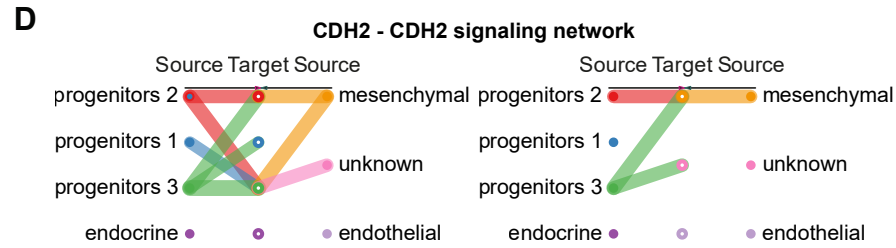


Figure S11. Overview of cell interactions between all clusters. (A) Number of interactions displaying how many ligand-receptor pairs are involved in cell-cell communication. The line thickness correlates with the number of ligand-receptor pairs. The circle width resembles the number of cells involved in signaling. (B) Represents the intensity (probability) of cell-cell communication between the clusters. The interaction strength correlates with the thickness of the lines. (C) Circle plots showing Collagen and Laminin signaling pathway networks. Hierarchy plots displaying ligand-receptor signaling networks of (D) CDH2-CDH2 and CDH1-CDH1, (E) DSC2-DSG2, (G) CD46-JAG1, (I) PRSS1-PARD3, and (J) PTN-NCL. (F) GAS, (H) NOTCH, and (K) GDF signaling networks are shown as heatmap unraveling cluster-specific roles in sender, receiver, mediator or influencer. CDH1: cadherin 1; CDH2: cadherin 2; DSC2: desmocollin 2; DSG2: desmoglein 2; GAS: growth arrest specific; GDF: growth differentiation factor; NCL: nucleolin; PTN: pleiotrophin

Supplemental Table S5. Media compositions of separate PKC activator testing. Applied compounds are highlighted in green. Related to Figure 2E.

		Experiment number (PKC activator testing)				
		1	2	3	4	5
Stage 1a	BE1 + 0.1% BSA					
	1 day					
	100 ng/mL Activin A					
	2 μ M CHIR99021					
Stage 1b	BE1 + 0.1% BSA					
	2 days					
	100 ng/mL Activin A					
	5 ng/mL FGF2					
Stage 2	BE1 + 0.5% BSA					
	3 days					
	50 ng/mL FGF10					
	3 ng/mL Wnt3A					
	0.25 mM vitaminC					
Stage 3	BE3 + 2% BSA					
	3 days					
	PKC activator		0.1 μM ILV	0.33 μM ILV	0.5 μM ILV	0.5 μM TPPB
	0.25 μ M SANT-1					
	1 μ M retinoic acid					
	16 mM additional glucose (in total 18.4 mM)					
	0.5 μ M TPPB					
Stage 4	BE3 + 2% BSA					
	4 days					
	PKC activator	0.33 μM ILV	0.1 μM ILV	0.33 μM ILV	0.5 μM ILV	0.5 μM TPPB
	100 ng/mL EGF					
	10 mM nicotinamide					
	0.33 μ M Indolactam V					
	16 mM additional glucose (in total 18.4 mM)					
	0.25 μ M SANT-1					
	0.5 μ M TPPB					

References

1. M. Breunig, J. Merkle, M. K. Melzer, S. Heller, T. Seufferlein, M. Meier, M. Hohwieler, A. Kleger. Differentiation of human pluripotent stem cells into pancreatic duct-like organoids. *STAR Protoc* **2**, 100913 (2021).
2. M. Breunig, J. Merkle, M. Wagner, M. K. Melzer, T. F. E. Barth, T. Engleitner, J. Krumm, S. Wiedenmann, C. M. Cohrs, L. Perkhofer *et al.* Modeling plasticity and dysplasia of pancreatic ductal organoids derived from human pluripotent stem cells. *Cell Stem Cell* **28**, 1105-1124 e1119 (2021).
3. M. Hohwieler, A. Illing, P. C. Hermann, T. Mayer, M. Stockmann, L. Perkhofer, T. Eiseler, J. S. Antony, M. Muller, S. Renz *et al.* Human pluripotent stem cell-derived acinar/ductal organoids generate human pancreas upon orthotopic transplantation and allow disease modelling. *Gut* **66**, 473-486 (2017).
4. N. J. Hoglebe, K. G. Maxwell, P. Augsornworawat, J. R. Millman. Generation of insulin-producing pancreatic beta cells from multiple human stem cell lines. *Nat Protoc* **16**, 4109-4143 (2021).
5. N. C. Leite, E. Sintov, T. B. Meissner, M. A. Brehm, D. L. Greiner, D. M. Harlan, D. A. Melton. Modeling Type 1 Diabetes In Vitro Using Human Pluripotent Stem Cells. *Cell Rep* **32**, 107894 (2020).
6. P. U. Mahaddalkar, K. Scheibner, S. Pfluger, Ansarullah, M. Sterr, J. Beckenbauer, M. Irmeler, J. Beckers, S. Knobel, H. Lickert. Generation of pancreatic beta cells from CD177(+) anterior definitive endoderm. *Nat Biotechnol* **38**, 1061-1072 (2020).
7. N. J. Hoglebe, P. Augsornworawat, K. G. Maxwell, L. Velazco-Cruz, J. R. Millman. Targeting the cytoskeleton to direct pancreatic differentiation of human pluripotent stem cells. *Nat Biotechnol* **38**, 460-470 (2020).